Aree naturali protette e buon governo del territorio. Il Piano d’area del Parco Naturale del Po piemontese, tra eredità e innovazione

On the Information Carried by Correlated Collaborative Ranging Measurements for Hybrid Positioning

Alex Minetto, *Student Member, IEEE*, and Fabio Dovis, *Member, IEEE*

***Abstract*—Previous research contributions have addressed the definition of a Cramer Rao Lower Bound (CRLB) to investigate the performance of hybrid positioning algorithms that exploit satellite-based range measurements and independent terrestrial range measurements. Starting from such results, this work investigates the quantity of information carried by terrestrial relative measurements obtained from the combination of satellite-based range measurements shared among pairs of connected agents. The study is conceived to investigate the impact of such relative ranges on the positioning error when they are used as additional measurements to help improving accuracy and precision of positioning. By considering some prior knowledge about satellite-to-user and user-to-user ranging uncertainties, the approximation of a theoretical limit for this novel class of hybrid positioning algorithms allows to observe when the use of cooperative ranges is beneficial, depending on their variance and on the geometry of satellites and terrestrial agents.**

***Index Terms*—Global navigation satellite system, global positioning system, cramer-rao bounds, cooperative systems, multi-agent systems.**

I. Introduction

PREVIOUS works in the field of collaborative positioning demonstrated that the estimation of the positioning solution can be improved by merging different range information from known reference points such as satellites, terrestrial anchors, peer agents and signals of opportunity [1]–[5]. As a target application, this hybrid positioning approach has been extensively exploited to improve availability, accuracy and precision of Global Navigation Satellite Systems (GNSS) [6].

In the last decade theoretical limits of cooperative positioning have been investigated in several works by mainly considering independent measurement contributions. For example, in [7], [8] the authors first investigate the problem for sensor networks applications, in [9], [10] an exhaustive theoretical analysis on the topic is provided for networks of cooperative users and in [11] the authors have derived the Cramer Rao Lower Bound (CRLB) for generic hybrid cooperative solutions. Recently, the research about theoretical limits of cooperative positioning has became appealing in the field of Intelligent Transportation Systems, thus rising a new interest to the topic [12], [13].

The measurements have been typically assumed to be statistically independent and Gaussian distributed such that their uncorrelation has been assessed by definition [14]. As a consequence, it has been shown that under these assumptions the overall quantity of information carried by the measurements is simply the sum of the independent information contributions.

Cooperative positioning is hence known to be beneficial against GNSS impairments and to generally improve accuracy [15]–[18] but less research effort has been spent in showing that the combination of satellite-based and correlated terrestrial measurements can still bring benefits in terms of quantity of information about the estimated position. Nevertheless, a theoretical investigation which justifies this additional information is still missing. In light of this, other works extended the definition of Geometrical Dilution of Precision to auxiliary collaborative contributions by demonstrating the related effects on the positioning error [15], [19]. They pursued the definition of an overall multiplicative factor by facing the problem from a theoretical perspective without addressing any specific ranging method or technology.

Recent cooperative approaches aim at combining both computational effort and navigation data from swarms of networked agents to support the increasing demand for reliable positioning and navigation capabilities [20], [21]. The use of measurements such as GNSS-based ranging [22]–[24] implies a correlation among the measurements involved in the positioning problem, thus weakening the conditions which are tipically assumed for the computation of the related theoretical limits. Such a correlation is either due to the use of the estimated position or to the measurements combination exploited in several ranging algorithms (see for example [22], [25]). Furthermore, the statistical properties of such kind of measurements are not well-defined in literature due to their strong dependencies on the geometrical configuration of the experiments.

Despite these drawbacks, numerical simulations documented in this paper returned remarkable improvement of the hybrid positioning solution w.r.t. a standalone GNSS approach both in terms of precision and accuracy. The Cramer Rao Lower Bound (CRLB) computed for hybrid cooperative positioning has been used to estimate the variance of a hybrid Least Mean Square (LMS) estimator based on correlated input measurements and

Manuscript received January 2, 2019; revised May 16, 2019 and July 30, 2019; accepted November 26, 2019. Date of publication December 6, 2019; date of current version February 12, 2020. The review of this article was coordinated by Prof. J. F. Paris *(Corresponding author: Alex Minetto.)*

The authors are with the Department of Electronics and Telecommunications, Politecnico di Torino, 10129 Torino, Italy (e-mail: alex.minetto@polito.it; fabio.dovis@polito.it).

Digital Object Identifier 10.1109/TVT.2019.2957015

it has been observed that its behaviour still has an appreciable match with the simulation results.

The paper is organized as follows: Section II introduces relevant fundamentals about the characterization of the positioning error and illustrates the basics modelling of the involved measurements; Section III recalls the derivation of the Fisher Information for the position estimation; Section IV describes the simulation environment and metrics. Eventually, Section V discusses numerical results obtained through a meaningful dynamic example and a set of simple geometrical trajectories.

II. Background

The amount of information carried by an observed unbiased range measurement w.r.t. the estimated position is related to the relative position of the reference points and to the quality of the observable measurements [26]. The goodness of this information is indeed inversely proportional to the variance of the measurement error itself. On the other hand, the range direction leads to a fundamental issue known as Geometrical Dilution Of Precision (GDOP) [27]. The GDOP affects the positioning solution by altering the shape of the spatial distributions of its realizations, namely its precision which is evaluated through the *position error covariance matrix*. The combination of the variance of such measurements and the GDOP characterizes the whole positioning error, derived as in [28] from the Cramer Rao Lower Bound of the positioning estimator.

In light of this, the analysis presented in [19] investigates a composite dilution of precision for cooperative positioning, named Collaborative Dilution Of Precision (CDOP), by including generic terrestrial ranging contributions in the measurements set available for the computation of the position. The study provides a demonstration of a fundamental result by stating that CDOP $\leq$ GDOP. As it has been demonstrated for satellite-based navigation, any additional range contribution provided w.r.t. terrestrial reference points cannot increase the geometrical dilution factor. However, the variance of the estimated position depends also on the error contribution affecting the measurements. The analysis of the CRLB for a position estimator hence allows to include all the measurements uncertainties in the evaluation of the profitability of GNSS-based hybrid collaborative navigation.

A. The Fisher Information and the Cramer Rao Lower Bound

The CRLB is employed to identify the minimum variance that can be reached by a given unbiased estimator [14]. Indeed, the related Cramer Rao inequality states that this variance is bounded by the inverse of the *Fisher Information* carried by the observable set of measurements $\boldsymbol{\mu}$. This fundamental limit can be generalized in its matrix form, as

$$[\mathbf{P}_{\boldsymbol{\theta}}]_{i,j} \geq [\mathbf{F}_{\boldsymbol{\theta}}]^{-1}_{i,j} = \left[-\mathbf{E}\left(\frac{\partial^2}{\partial\theta_i \partial\theta_j} \log f\left(\boldsymbol{\mu};\boldsymbol{\theta}\right)\Big|_{\boldsymbol{\theta}} \right) \right]^{-1} \quad (1)$$

where the pair (i, j) identifies the element of the matrix located at the i-th row and j-th column, $\boldsymbol{\theta} = [\,\theta_1, \theta_2, \ldots, \theta_M\,]^T$ is a $M \times 1$ vector which defines the target state, and $\boldsymbol{\mu}$ is the observed realization of a multivariate measurements vector which is associated to $\boldsymbol{\theta}$ by means of the Probability Density Function (PDF) $f(\boldsymbol{\mu};\boldsymbol{\theta})$. The $\mathbf{F}_{\boldsymbol{\theta}}$ is a $M \times M$ matrix named *Fisher Information Matrix* (FIM) and its inverse is namely the CRLB matrix.

Given that both $\mathbf{P}_{\hat{\boldsymbol{\theta}}}$ and $[\mathbf{F}_{\boldsymbol{\theta}}]^{-1}$ are positive definite, an ordering relation can be defined to compare two estimators $T(\boldsymbol{\mu})$ and $T'(\boldsymbol{\mu})$, as

$$[\mathbf{F}_{T,\boldsymbol{\theta}}]^{-1} > [\mathbf{F}_{T,'\boldsymbol{\theta}}]^{-1} \longrightarrow \mathrm{Tr}\left([\mathbf{F}_{T,\boldsymbol{\theta}}]^{-1}\right) > \mathrm{Tr}\left([\mathbf{F}_{T,'\boldsymbol{\theta}}]^{-1}\right) \quad (2)$$

where $\mathrm{Tr}(\cdot)$ is the trace operand which sums the diagonal elements of a given matrix.

When unbiased estimators are considered, the comparison of the respective CRLBs (1) allows to identify the most advantageous solution.

This study, starting from the definition of the CRLB for hybrid positioning obtained under realistic assumptions, shows how a terrestrial correlated range brings information to the position estimation process depending on the observation conditions.

B. Range Contributions Modelling

In this study, two classes of range measurements are identified as observable variables of the measurement vector, $\boldsymbol{\mu}$, in (1). They are defined w.r.t. the *target agent*, m, located at $\mathbf{x}_m$:

- $\hat{\rho}_{s,m}(t_k)$ is an estimate of the *pseudorange* between the agent m and the satellite s at a given instant t_k [26], defined as

$$\hat{\rho}_{s,m}(t_k) = ||\mathbf{x}_s(t_k) - \mathbf{x}_m(t_k)|| + b_m(t_k) + \nu_{s,m}(t_k) \quad (3)$$

  where $\mathbf{x}_s(t_k)$ is the position of the satellite, $b_m(t_k)$ is a bias term due to the clocks misalignment and $\nu_{s,m}(t_k)$ is the noise due to residual errors affecting the measurements [26]. It is assumed Gaussian-distributed with zero-mean and variance $\sigma^2_{s,m}(t_k)$.
- $\hat{\delta}_{n,m}(t_k)$ is an estimate of a pseudo inter-agent distance between the terrestrial agents m and n

$$\hat{\delta}_{n,m}(t_k) = ||\mathbf{x}_n(t_k) - \mathbf{x}_m(t_k)|| + b_{n,m}(t_k) + \nu_{n,m}(t_k) \quad (4)$$

  where $\mathbf{x}_n(t_k)$ is the position of the agent n, $b_{n,m}(t_k)$ is a generic bias term due to the ranging technique and $\nu_{n,m}(t_k)$ is the additive noise term affecting the measurements. For simplicity, as for the first class, it is assumed Gaussian-distributed with zero-mean and variance $\sigma^2_{n,m}(t_k)$ but its distribution can vary according to the range computation methods (e.g. single difference, double difference, raw pseudorange ranging) [22].

Let consider multiple ranges are expected to be obtained for each class assuming that measurements coming from the same class are independent. According to this assumption their error covariance matrices are diagonal and defined as $\mathbf{R}_\rho(t_k) = \mathbf{E}[\boldsymbol{\rho}(t_k)\boldsymbol{\rho}(t_k)^T]$ and $\mathbf{R}_\delta(t_k) = \mathbf{E}[\boldsymbol{\delta}(t_k)\boldsymbol{\delta}(t_k)^T]$ where $\boldsymbol{\rho}(t_k)$ and $\boldsymbol{\delta}(t_k)$ are generic *measurements vectors* composed by a set of S and N range measurements from each class, respectively. A hybrid positioning solution combines the column vectors $\boldsymbol{\rho}(t_k)$ and $\boldsymbol{\delta}(t_k)$ in a *hybrid measurements vector*,

$$\boldsymbol{\mu}_m(t_k) = \left[\, \boldsymbol{\rho}_m(t_k)^T \; \boldsymbol{\delta}_m(t_k)^T \,\right]^T \quad (5)$$

and the related *measurements noise covariance matrix* is hence defined as

$$\mathbf{R}_{\boldsymbol{\mu}}(t_k) = \begin{bmatrix} \mathbf{R}_d(t_k) & \mathbf{R}_{dr}(t_k) \\ \mathbf{R}_{rd}(t_k) & \mathbf{R}_r(t_k) \end{bmatrix} \tag{6}$$

where the sub-matrices $\mathbf{R}_{rd}(t_k) = \mathbf{R}_{dr}(t_k) = \underline{\mathbf{0}}$ if and only if terrestrial ranges are obtained independently from satellite-ranges included in $\boldsymbol{\mu}(t_k)$. This specific case has been heavily investigated for hybrid positioning with ranging sensors [11], [15] while in this study this restrictive assumption is relaxed.

C. Position Estimation and Error Covariance Matrix

In this work, the estimation of the position is performed by means of a LMS approach, which is a Best Linear Unbiased Estimator (BLUE) for Gaussian inputs [14]. It is largerly used for the solution of the trilateration problem in positioning and navigation to retrieve the Position, Time and Velocity (PVT) solution [26]. Given a linearization point, $\mathbf{x}_0$, the positioning solution can be computed iteratively as $[\hat{\mathbf{x}}_m(t_k) \quad \hat{b}_m(t_k)]^T = [\mathbf{x}_0 \quad b_0]^T + [\Delta\hat{\mathbf{x}}_m(t_k) \quad \Delta\hat{b}_m(t_k)]^T$ where the last term is given by

$$\begin{bmatrix} [\Delta\hat{\mathbf{x}}_m(t_k)]^T \\ \Delta\hat{b}_m(t_k) \end{bmatrix} = (\mathbf{H}^T\mathbf{H})^{-1}\mathbf{H}^T\Delta\boldsymbol{\mu}_m(t_k) \tag{7}$$

where $\mathbf{H}$ is the *direct cosine matrix* whose generic s-th row is defined as,

$$[\mathbf{H}]_s = \left[(\mathbf{x}_s - \hat{\mathbf{x}}_m) / ||\mathbf{x}_s - \hat{\mathbf{x}}_m|| \; 1 \right] = \left[\mathbf{h}_{s,m} \; 1 \right] \tag{8}$$

and $\mathbf{h}_{s,m}$ is the *unitary steering vector* pointing towards the s-th satellite. Each positioning solution, $\hat{\mathbf{x}}_m(t_k)$, is independent from the previous one, $\hat{\mathbf{x}}_m(t_k - 1)$.

Assuming a simple statistical model of zero-mean i.i.d. for the satellite range measurements in $\boldsymbol{\mu}_m$, the error covariance matrix of the position estimate is defined as

$$\mathbf{P}_\theta = \sigma_\mu^2 \left(\mathbf{H}^{\mathrm{T}}\mathbf{H}\right)^{-1} \tag{9}$$

where σ_μ^2 is the variance of the measurements. The GDOP is then suitable to the computation of the Root Mean Square error of the positioning solution but according to the definition, only the diagonal terms of (9) are considered. Differently from the GDOP, the FIM allows to investigate correlations among the errors according to the non-diagonal terms of the error covariance matrix.

III. Fisher Information Matrix in Positioning Estimation

As in (1), in order to evaluate the FIM it is sufficient to compute the second order derivative of the logarithm of the likelihood w.r.t. the column vector $\boldsymbol{\theta}(t_k)$, were

$$\boldsymbol{\theta}(t_k) = \left[\mathbf{x}_m(t_k) \; b_m(t_k) \right]^T. \tag{10}$$

In order to focus on the improvement of accuracy and precision of the positioning estimate, the bias term, $b_m(t_k)$, will be eventually dropped as it is compensated from previous solutions $\hat{\boldsymbol{\theta}}(t_{k-1})$, being functional to the position computation [26]. In the following derivation, time index will be dropped as well for readability reasons.

A. Fisher Information Matrix for Satellite-Only Contributions

The theoretical log-likelihood for a generic Gaussian random variable is defined as

$$\mathcal{L}(\theta, \rho, \sigma_i) = \log \frac{1}{\sqrt{2\pi}\sigma_i} - \frac{1}{2}\frac{(\mathbf{x} - \theta)^2}{\sigma_i^2}. \tag{11}$$

Consequently, the log likelihood for a Gaussian pseudorange measured from a generic satellite, s, is obtained as

$$\begin{aligned} \mathcal{L}(\mathbf{x}_m, r_{s,m}, \sigma_{s,m}) &= \log p(\hat{\rho}_{s,m} | x_m, b_m) \\ &= C - \frac{|\hat{\rho}_{s,m} - ||\mathbf{x}_s - \mathbf{x}_m|| - b_m|^2}{2\sigma_{s,m}^2} \end{aligned} \tag{12}$$

where C is the constant term resulting from the first term of the summation in (11), and $\sigma_{s,m}$ is the standard deviation associated to the pseudorange measurement $\hat{\rho}_{s,m}$.

As shown in [11], the FIM is computed as

$$\mathbf{F}_m = -\mathbf{E}\left\{ H_m \left[\sum_s^{S_m} \mathcal{L}(\mathbf{x}_m, r_{s,m}, \sigma_{s,m}) \right] \right\} \tag{13}$$

where H_m is the Hessian operator of the second order partial derivatives. The FIM is hence defined as

$$\mathbf{F}_m = \begin{bmatrix} \mathbf{F}_{\mathbf{x}_m} & \mathbf{f}_{x_m,b_m} \\ \mathbf{f}_{x_m,b_m}^T & F_{b_m} \end{bmatrix} \tag{14}$$

where each submatrix can be computed as

$$\mathbf{F}_{\mathbf{x}_m} = \sum_{s \in \mathcal{S}_m} \frac{1}{\sigma_{s,m}^2} \mathbf{h}_{s,m}\mathbf{h}_{s,m}^T \tag{15}$$

$$F_{b_m} = \sum_{s \in \mathcal{S}_m} \frac{1}{\sigma_{s,m}^2} \tag{16}$$

$$\mathbf{f}_{\mathbf{x}_m,b_m}^T = \sum_{s \in \mathcal{S}_m} -\frac{1}{\sigma_{s,m}^2} \mathbf{h}_{s,m}. \tag{17}$$

where S_m indicates the set of satellites used by the target agent, m, to compute its PVT.

B. Fisher Information Matrix for Cooperative Contributions

For the sake of simplicity, an estimate of a terrestrial range, $\hat{d}_{n,m}(t_k) = \hat{\delta}_{n,m}(t_k) - b_m(t_k)$, is considered by means of Inter-Agent Range (IAR) algorithm [25], here recalled as

$$\hat{I}_{n,m}^s = \sqrt{\hat{r}_{s,m}^2 + \hat{r}_{s,n}^2 - 2\hat{r}_{s,n}\hat{r}_{s,m}(\mathbf{h}_{s,m} \cdot \mathbf{h}_{s,n})} \tag{18}$$

where $\hat{r}_{s,m} = \hat{\rho}_{s,m} - b_m$ and $\hat{r}_{s,n} = \hat{\rho}_{s,n} - b_n$. Given multiple shareable satellites between the collaborating agents, the $\hat{d}_{n,m}$ can be computed as the weighted average of a set of contributions, as

$$\hat{d}_{n,m} = \sum_{s=1}^{S} w_s \hat{I}_{n,m}^s \tag{19}$$

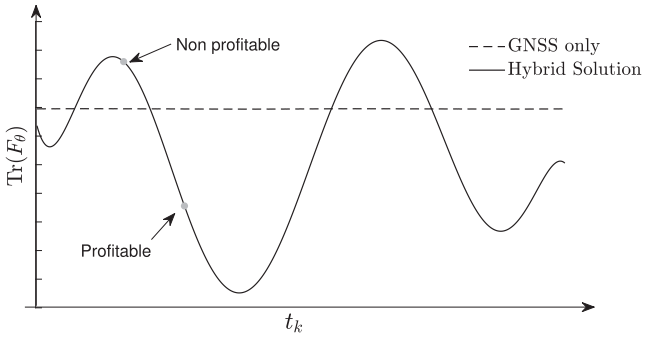

Fig. 1. Example of theoretical computation of satellite-based positioning CRLB vs. hybrid positioning CRLB for a dynamic trajectory.

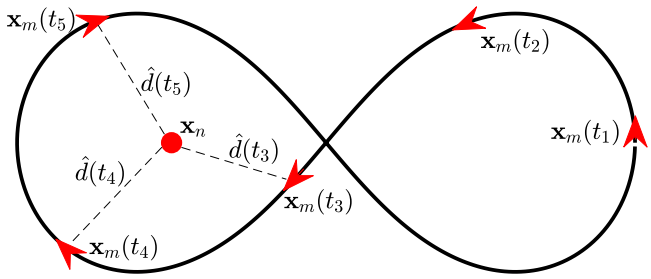

Fig. 2. Example of a Bernoullian lemniscate path of 1046.7 m travelled at an average speed of 26.15 m/s. The dashed lines show the additional terrestrial range provided according to (18).

where the terms w_s are the weights attributed to each measurement according to its variance. Although it has been shown that IAR is characterized by a Gaussian-like distribution, its statistics is very sensitive to geometrical conditions [29]. By neglecting on purpose this peculiar behaviour, the same approach discussed for the evaluation of the FIM about satellite range measurements is applied to the likelihood defined for GNSS-only collaboratively-computed range measurements

$$\log p\left(\hat{d}_{n,m}|x_m\right) = C - \frac{|\hat{d}_{n,m} - ||\mathbf{x}_n - \mathbf{x}_m|| - b_{n,m}|^2}{2\sigma^2_{n,m}}. \tag{20}$$

Therefore, (13) is applied to (20) neglecting any dependency with respect to the other measurements. Eventually, the $\mathbf{F}_m$ for the hybrid system is still computed according to (14).

C. On the Approximation of the FIM for Hybrid Positioning Solutions

Actually, the CRLB of the hybrid solution can be used as an estimation of the error covariance matrix of the hybrid position estimate. As proposed in [11], the hybrid FIM can be obtained by the sum of the satellite-only FIM and the cooperative FIM if and only if independent measurements are considered.

In order to deal with measurements correlation the FIM should be instead computed as $\mathbf{F}_{\boldsymbol{\theta},\boldsymbol{\mu}} = \mathbf{F}_{\boldsymbol{\theta},\boldsymbol{\rho}} + \mathbf{F}_{\boldsymbol{\theta},\boldsymbol{d}|\boldsymbol{\rho}}$, where $\mathbf{F}_{\boldsymbol{\theta},\boldsymbol{d}|\boldsymbol{\rho}}$ is the Fisher information related to the conditional probability density of the inter-agent range measurements for the given set of pseudoranges measurements, $\boldsymbol{\rho}$. The computation of the mutual Fisher information is out of the scope of this paper provided that the likelihood of the inter-agent range measurements must be derived specifically for any given geometrical conditions [29]. The proposed solution does not contemplate correlation among the two classes of measurements, therefore the hybrid FIM is obtained through the computation of (15), (16), (17) for all the available measurements in the hybrid measurement vector, $\boldsymbol{\mu}_m$. Although it is assumed that $\mathbf{F}_{\boldsymbol{\theta},\boldsymbol{d}|\boldsymbol{\rho}} \simeq \mathbf{F}_{\boldsymbol{\theta},\boldsymbol{d}}$, no remarkable losses were observed in terms of covariance estimation accuracy, as it will be shown in the results in Section V.

In the example shown in Figure 1, given a pre-defined trajectory and an a-priori knowledge of the measurements variances, the CRLB is expected to identify the profitable time instants in which cooperative approach guarantees improved precision w.r.t. GNSS standalone positioning.

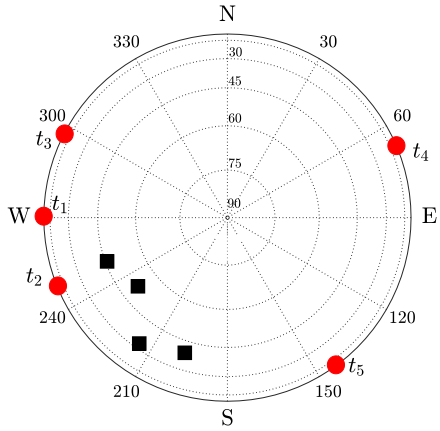

Fig. 3. Skyplot of the relative azimuth, ϕ, and elevation, α, of the satellites and the aiding agent w.r.t. the target agent position at given time instant.

Moving from these considerations and from the FIM derivation for the Gaussian-distributed satellite range measurements recalled so far, the same quantity is computed for correlated terrestrial range measurements to estimate and compare the overall uncertainty of the computed position estimates.

IV. Methodology

The proposed numerical simulation aims at analysing the impact on the positioning algorithm of the target agent which integrates correlated satellite and dependent terrestrial range measurements. Furthermore, the analysis aim at verifying whether an approximation of the CRLB can still be suitable to identify the profitability of the technique.

The target agent moves along the Bernoullian path in Figure 2 while the aiding agent position, $\mathbf{x}_n$ is assumed static for every t_k. In the considered scenario both the agents compute their position estimates, $\hat{\mathbf{x}}_n$ and $\hat{\mathbf{x}}_m$, by relying on a given set of satellites, depicted in Figure 3. The target agent is designed to exploit the IAR information obtained for each time instant, t_k through the collaboration with the aiding agent. As depicted in Figure 4, the GNSS-only positioning, referred to as LMS,

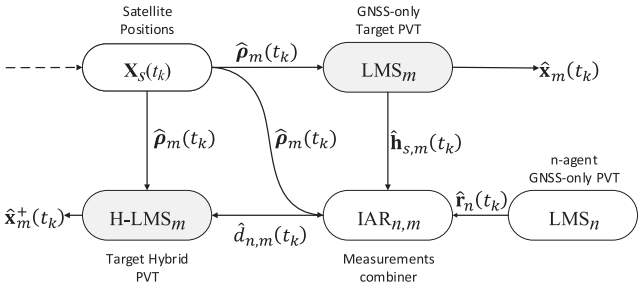

Fig. 4. Block scheme of numerical simulations. The outputs of the LMS blocks were compared to assess the positioning performance. $\mathbf{X_S}$ indicates the positions of the visible satellites.

is first performed to obtain a coarse estimate of $\hat{\mathbf{x}}_m(t_k)$, then navigation data are used to determine collaborative ranges $\hat{\mathbf{d}}_{n,m}(t_k)$ which are integrated in a further hybrid positioning computation, named H-LMS, to refine the previous outcome, hereafter referred as to $\hat{\mathbf{x}}_m^+(t_k)$.

For sake of example, 4 satellites with azimuth $\phi \in \{\pi, \frac{3}{2}\pi\}$ and elevation $\alpha \in \{\frac{\pi}{24}, \frac{\pi}{2}\}$ were considered. The axial standard deviations were measured from the numerical simulation and, in parallel, estimated through the CRLB (1).

The following analysis is based on a Monte Carlo simulation by consider W realizations of the trajectory followed by the moving agent. The IAR measurements are expected to vary along with the time, t_k, while satellites are assumed static to limit the variability of the scenario without any loss of generality. The measurement and the positioning estimates are performed for each run at the same time instant, t_k.

The error covariance matrix of each positioning solution is estimated as

$$\hat{\mathbf{P}}_x(t_k) = \frac{1}{W-1}\sum_{w=1}^{W}\left(\hat{\mathbf{x}}_w - \boldsymbol{\mu}\right)\left(\hat{\mathbf{x}}_w - \boldsymbol{\mu}\right)^T. \qquad (21)$$

In the following, the horizontal components of (21) are plotted as *information ellipses* [9] according to the eigenvalues of the position error covariance matrix. The positioning bias is computed as the mean error w.r.t. the true position of the target agent

$$\hat{\xi}_{\mathbf{x}}(t_k) = \frac{1}{W}\sum_{w=1}^{W}\left(\hat{\mathbf{x}}_w - \mathbf{x}\right). \qquad (22)$$

In order to observe the correlation of the measurements involved in the hybrid estimation of the position, the *Pearson correlation coefficients* of the measurements are computed as

$$C(\boldsymbol{\mu}_1(t_k), \boldsymbol{\mu}_2(t_k)) = \frac{\mathrm{cov}\left[\boldsymbol{\mu}_1(t_k), \boldsymbol{\mu}_2(t_k)\right]}{\sigma_{\boldsymbol{\mu}_1(t_k)}\sigma_{\boldsymbol{\mu}_2(t_k)}}. \qquad (23)$$

where $\mathrm{cov}(\cdot)$ indicates the same covariance estimator as for (9) and the generic $\boldsymbol{\mu}(t_k)$ collects a set of W random realizations of the measurements vector for the instant t_k.

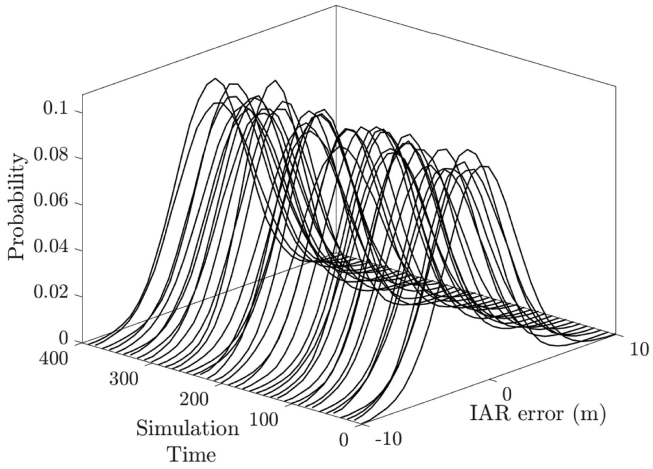

Fig. 5. Example of IAR error PDFs evaluated in a set of time instants along the Bernoullian trajectory.

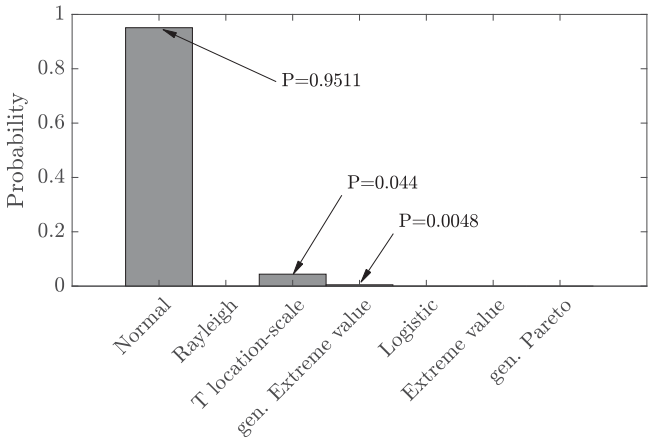

Fig. 6. Probability of BIC best fits of the IAR error w.r.t. to a set of known statistical distributions.

The profitability of the hybrid solution is evaluated by means of (2), as the ratio of the time instants t_k in which the condition

$$\mathrm{Tr}\left(\left[\mathbf{F}_{\text{H-LMS},\mathbf{x}}(t_k)\right]^{-1}\right) > \mathrm{Tr}\left(\left[\mathbf{F}_{\text{LMS},\mathbf{x}}(t_k)\right]^{-1}\right) \qquad (24)$$

is satisfied w.r.t. the overall simulation time. The *profitability percentage* of the methods will be referred to as τ_{exp} and τ_{CRLB} to describe the advantage of H-LMS computed from the numerical simulation and from CRLB, respectively.

V. Numerical Results

In this section, results from the aforementioned Bernoullian trajectory are first presented addressing a statistical analysis of the correlated measurements. The determination of the profitability of the H-LMS is then detailed by comparing the values obtained from numerical simulation and theoretical CRLB. A set of elementary trajectories is eventually tested to extend the analysis to a wider range of geometrical conditions for the target agent.

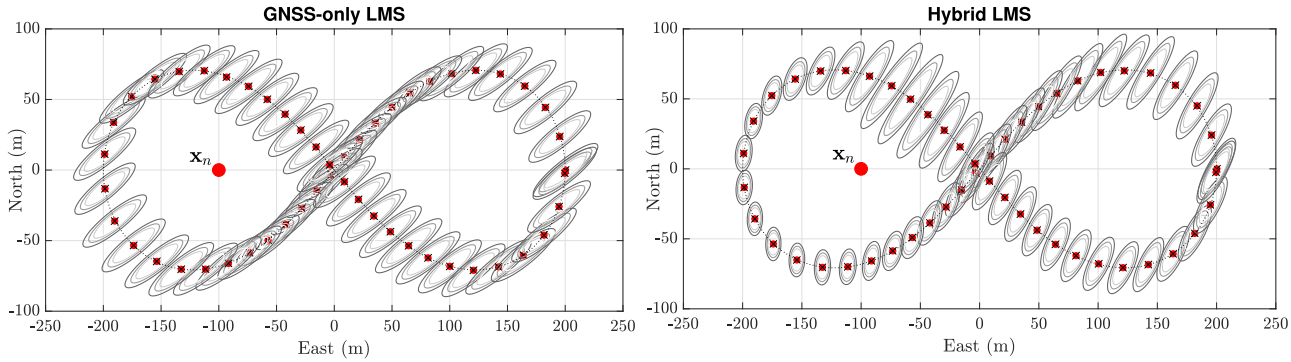

Fig. 7. Estimated positioning solutions according to the scenario in Figure 2. The information ellipses describe the horizontal standard deviation at 90%, 99% and 99.9% of confidence interval, obtained from the eigenvalues of the matrix $P_{\mathbf{x}}$ in a subset of time instants, t_k. Results from a Monte Carlo simulation with parameters $W = 10000$, $\sigma_{s,m} = 1$, $max(d_{n,m}) = 200$ m.

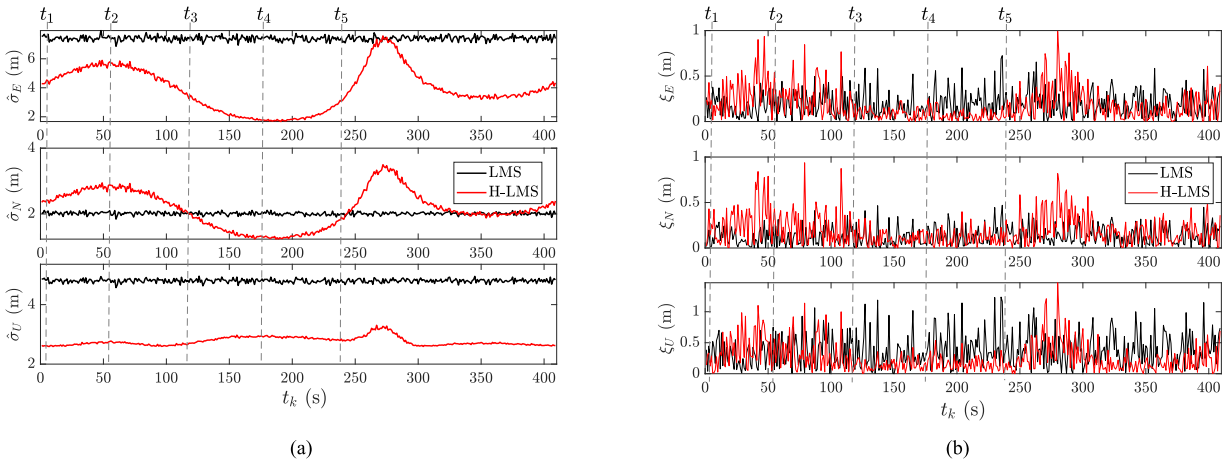

(a) (b)

Fig. 8. Statistical analysis of experimtal biases and standard deviations of standalone and hybrid positioning solutions by means of Monte Carlo simulations. (a) Axial standard deviations estimated according to (21). (b) Axial biases estimated according to (22).

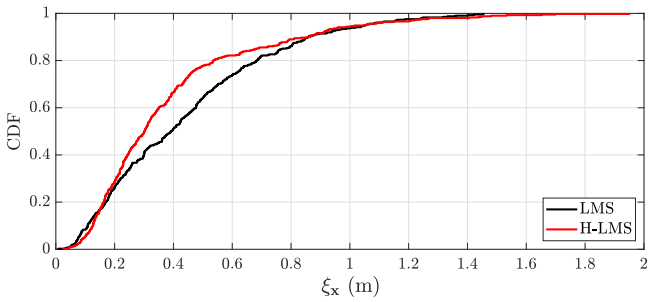

Fig. 9. Empirical Cumulative Density Function (CDF) of the positioning error $\hat{\xi}_{\mathbf{x}}$ for each time instant t_k.

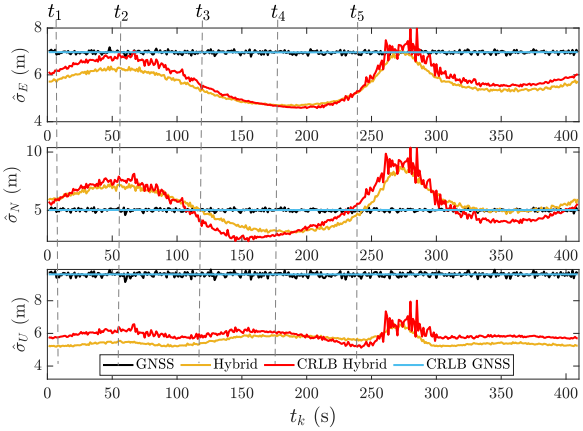

Fig. 10. Comparison of measured axial standard deviations and estimated standard deviations from the CRLB for LMS positioning and H-LMS by Monte Carlo simulations.

A. *Hybrid Positioning in Bernoullian Trajectory*

The results presented in this subsection are referred to the example of collaborative scenario depicted in Figure 2 and obtained by means of a Monte Carlo simulation using $W = 10000$ trials for each time instants t_k.

1) Statistics of Terrestrial Measurements: In order to justify the Gaussian likelihood (20) proposed in Section III to model the IAR contributions, an analysis on the statistical distribution of the collaborative range measurements has been performed. Figure 5 shows a time series of the statistical distributions of the IAR error w.r.t. the true distance between the target and

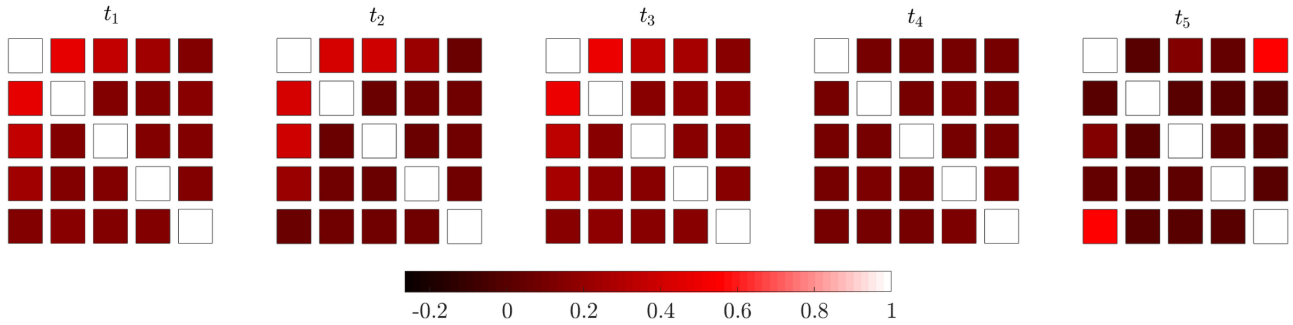

Fig. 11. Matrices of Pearson correlation coefficients (23) computed for the measurement error covariance $\mathbf{R}_\rho$, and observed at sample time instants t_k, where $k \in \{1, 5\}$.

aiding agents. It is relevant to consider that each IAR is computed according to a weighted average among the available satellites, as in (19).

It can be noticed how the qualitative plot of the statistic of the IAR PDFs resembles, for the largest part of the time, a Gaussian distribution.

This is confirmed by a full quantitative analysis based on a *Bayesian Information Criterion* (BIC), used to classify the error distribution of the IAR measurements. In Figure 6, the histogram indicates the normalized occurrences of each fit test. It can be shown that the ranging error is mostly normally distributed (95.11% of the overall simulation time), thus supporting the approximation proposed for the evaluation of the CRLB for a considerable set of time instants, t_k. Provided that a BIC analysis relies on the maximization of the likelihood for a set of observations, this result strongly supports the choice of a Gaussian likelihood in the FIM computation also for the elements related to the IAR measurements. Other distributions can be seen fitting the error statistics with a negligible probability.

2) Hybrid Positioning With Correlated Measurements: In Figure 7, the positioning solution of the LMS (left) and H-LMS (right) are presented. The information ellipses shows a remarkable difference between the two approaches in terms of error covariance matrix of the positioning solution. The most significant improvement can be observed between the time instants t_3 and t_5. It is evident from the plots that the hybrid solution integrating IAR measurements reduces the uncertainty in some specific portions of the path. The cumulative density function of the Root Mean Square Error (RMSE), computed along the trajectory presented in Figure 9, shows that the hybrid scheme overall improves the positioning performance w.r.t. GNSS standalone solution. The time series of axial biases and standard deviations are reported in Figure 8 a and Figure 8 b, respectively. It is worth to noticing that both the metrics show a higher dynamics for the hybrid solution due to the fast variations in the relative positions of the agents w.r.t. the slower satellites-to-target dynamics. By considering the standard deviation behaviour depicted in Figure 8 a, it is remarkable that on y-axis the aforementioned improvement is still well visible between t_3 and t_5, when the collaborating agent is observed in the opposite direction w.r.t. the satellites. The z-axis is instead less sensitive to the dynamics of the agents since their relative elevation does not vary along the trajectory. As shown in Figure 8 b, also the bias presents a similar behaviour, showing improved performance according to the same favourable position of the collaborating agent, $\mathbf{x}_n$.

The plots in Figure 11 shows the Pearson correlation coefficients (23) of the measurements at the different time instants t_k. The first row and column of each matrix indicates the correlation coefficients related to the dependent IAR measurement. It can be observed that in correspondence to t_4, a-posteriori identified as the most beneficial time-instant for cooperation, a very low correlation can be observed among the measurements.

To observe the benefits of H-LMS from the theoretical point of view, Figure 10 shows the comparison of the standard deviation computed via numerical simulation and the estimated ones obtained for the CRLB estimation of both the solutions. While the quantities match perfectly in the case of LMS, CRLB is not accurate for H-LMS due to the measurement correlation among IAR and pseudorange measurements. In correspondence of t_4, where the lowest correlation value has been observed, numerical values and theoretical estimations tends to match.

The profitability percentage in terms of horizontal precision of the H-LMS is evaluated computing the percentage of the time in which the trace of the covariance matrices and the CRLB of the H-LMS are lower than the respective values from the LMS. The profitability percentage computed by means of estimated CRLBs is 91.93%, which is remarkably close to the value obtained from simulated data, 89.73%.

Provided a coarse knowledge of the position of the collaborating agents and of the uncertainties of their GNSS measurements, an estimation of the uncertainty of the collaborative ranges can be in turn computed [29]. Finally, the approximation of the CRLB for the hybrid positioning algorithm can be used to enable hybrid positioning according to (2) or to exclude unprofitable terrestrial contributions through the minimization of the CRLB, as in [8].

B. Other Trajectories

The same scenario in terms of satellites and aiding agent locations is used to analyse a set of different trajectories to identify the profitable behaviour of the hybrid solution with different geometrical configurations. All the trajectories are centered around the origin of the simulated scenario.

TABLE I
COMPARISON OF PROFITABILITY OF H-LMS FOR OTHER ELEMENTARY GEOMETRICAL TRAJECTORIES

Trajectory Shape	τ_{exp}	τ_{CRLB}	MSE (m)
Squircle	72.21%	81.90%	0.26
Circular	73.11%	79.46%	0.21
Rose lemniscate	74.57%	77.50%	0.16
Archimedea Spiral	75.41%	80.67%	0.13
Bernoullian lemniscate	89.73%	91.93%	0.15

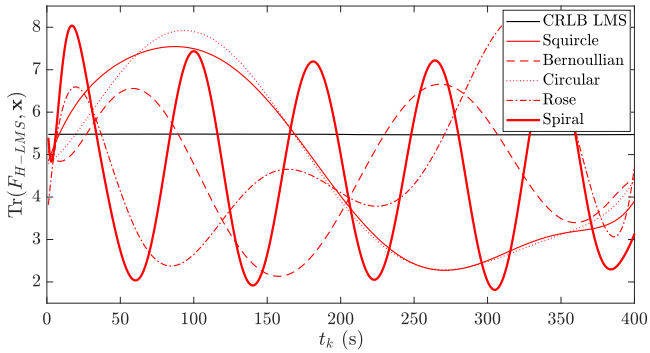

Fig. 12. Horizontal CRLB computed for H-LMS in different elementary geometrical trajectories vs. horizontal CRLB computed for LMS.

As shown in Table I, the evaluation of the profitability percentage, τ_{CRLB}, through the proposed estimation is more conservative w.r.t. the actual simulation results. Furthermore, the Mean Square Error (MSE) computed along the trajectory between simulated and theoretical standard deviation value is almost negligible for all the tested trajectories. Figure 12 summarizes the horizontal values of the theoretical CRLB computed for the H-LMS using different geometrical trajectories. The values are compared to the CRLB computed for LMS which is almost constant along all the trajectories due to the large distance of the satellites from the target at each t_k.

VI. CONCLUSION

Under proper conditions, the hybridization of satellite-based and dependent terrestrial measurements can increase the performance of standalone GNSS positioning similarly to the integration of independent terrestrial ranging contributions. In particular, when the geometry of the visible satellites is poor, as investigated in Section V, the additional information provided by collaborating agents mostly compensates for the dilution of precision.

The non-linear formula employed for the IAR computation between the two agents returns non-independent non-Gaussian range measurements whose distribution does not always match with the estimation model employed in LMS and used to derive the related CRLB (20). In these cases the simulated standard deviation can be lower than the CRLB as shown in the example discussed in Section V. This results are supported by the theory related to biased estimators and stability conditions of the CRLB.

The relevance of the presented results is threefold. On one side it has been shown that non-independent measurements can bring information to the positioning estimation. Furthermore, the simplistic usage of the likelihood function for Gaussian distributed variables with IAR measurements shows that their distribution cannot be Gaussian, thus leading to overoptimistic and over-pessimistic outcomes mainly depending on pseudoranges quality and geometry of the collaborating agents. In the end, the advantage of the proposed hybrid positioning strictly depends on the combined geometry and quality of the terrestrial ranging information and satellites constellation. Summarizing, relying on a proper knowledge of the measurements uncertainties, the used likelihoods definition and the related CRLB for the hybridization of cooperative range measurements can be used as an approximation of the expected position error covariance matrix to determine whether GNSS-based inter-agent collaboration can improve navigation and positioning performances.

REFERENCES

[1] D. Dardari, E. Falletti, and M. Luise, *Satellite and Terrestrial Radio Positioning Techniques: A Signal Processing Perspective*. New York, NY, USA: Academic, 2012.
[2] S. Frattasi and F. Della Rosa, *Mobile Positioning and Tracking: From Conventional to Cooperative Techniques*. Hoboken, NJ, USA: Wiley, 2017.
[3] Z. M. Kassas and T. E. Humphreys, "Observability analysis of collaborative opportunistic navigation with pseudorange measurements," *IEEE Trans. Intell. Transp. Syst.*, vol. 15, no. 1, pp. 260–273, Feb. 2014.
[4] J. Khalife and Z. M. Kassas, "Navigation with cellular CDMA signals—Part II: Performance analysis and experimental results," *IEEE Trans. Signal Process.*, vol. 66, no. 8, pp. 2204–2218, Apr. 2018.
[5] K. Shamaei, J. Khalife, and Z. M. Kassas, "Exploiting LTE signals for navigation: Theory to implementation," *IEEE Trans. Wireless Commun.*, vol. 17, no. 4, pp. 2173–2189, Apr. 2018.
[6] K. Liu, H. B. Lim, E. Frazzoli, H. Ji, and V. C. S. Lee, "Improving positioning accuracy using GPS pseudorange measurements for cooperative vehicular localization," *IEEE Trans. Veh. Technol.*, vol. 63, no. 6, pp. 2544–2556, Jul. 2014.
[7] E. G. Larsson, "Cramer-Rao bound analysis of distributed positioning in sensor networks," *IEEE Signal Process. Lett.*, vol. 11, no. 3, pp. 334–337, Mar. 2004.
[8] K. Das and H. Wymeersch, "Censoring for Bayesian cooperative positioning in dense wireless networks," *IEEE J. Sel. Areas Commun.*, vol. 30, no. 9, pp. 1835–1842, Oct. 2012.
[9] Y. Shen and M. Z. Win, "Fundamental limits of wideband localization—Part I: A general framework," *IEEE Trans. Inf. Theory*, vol. 56, no. 10, pp. 4956–4980, Oct. 2010.
[10] Y. Shen, H. Wymeersch, and M. Z. Win, "Fundamental limits of wideband localization—Part II: Cooperative networks," *IEEE Trans. Inf. Theory*, vol. 56, no. 10, pp. 4981–5000, Oct. 2010.
[11] F. Penna, M. A. Caceres, and H. Wymeersch, "Cramr-Rao bound for hybrid gnss-terrestrial cooperative positioning," *IEEE Commun. Lett.*, vol. 14, no. 11, pp. 1005–1007, Nov. 2010.
[12] J. Gabela, S. Goel, A. Kealy, M. Hedley, B. Moran, and S. Williams, "Cramér Rao bound analysis for cooperative positioning in intelligent transportation systems," in *Proc. Conf. Int. Global Navigat. Satell. Syst.*, Sydney, Australia, 2018, pp. 7–9.
[13] V. Gikas, G. Retscher, and A. Kealy, "Collaborative positioning for urban intelligent transportation systems (ITS) and personal mobility (PM): Challenges and perspectives," in *Mobility Patterns, Big Data and Transport Analytics*. New York, NY, USA: Elsevier, 2019, pp. 381–414.
[14] S. M. Kay, *Fundamentals of Statistical Signal Processing Estimation Theory*, vol. I. Upper Saddle River, NJ, USA: Prentice-Hall. 1993.

[15] G. M. Hoang, B. Denis, J. Hrri, and D. T. M. Slock, "Mitigating unbalanced GDoP effects in range-based vehicular cooperative localization," in *Proc. IEEE Int. Conf. Commun. Workshops*, May 2017, pp. 659–664.
[16] K. Liu, H. B. Lim, E. Frazzoli, H. Ji, and V. C. S. Lee, "Improving positioning accuracy using GPS pseudorange measurements for cooperative vehicular localization," *IEEE Trans. Veh. Technol.*, vol. 63, no. 6, pp. 2544–2556, Jul. 2014.
[17] N. Alam, A. T. Balaei, and A. G. Dempster, "A DSRC Doppler-based cooperative positioning enhancement for vehicular networks with GPS availability," *IEEE Trans. Veh. Technol.*, vol. 60, no. 9, pp. 4462–4470, Nov. 2011.
[18] N. Alam, A. T. Balaei, and A. G. Dempster, "Relative positioning enhancement in vanets: A tight integration approach," *IEEE Trans. Intell. Transp. Syst.*, vol. 14, no. 1, pp. 47–55, Mar. 2013.
[19] B. Huang, Z. Yao, X. Cui, and M. Lu, "Dilution of precision analysis for GNSS collaborative positioning," *IEEE Trans. Veh. Technol.*, vol. 65, no. 5, pp. 3401–3415, May 2016.
[20] U. Niesen, V. N. Ekambaram, J. Jose, and X. Wu, "Intervehicle range estimation from periodic broadcasts," *IEEE Trans. Veh. Technol.*, vol. 66, no. 12, pp. 10 637–10 646, Dec. 2017.
[21] F. Shen, J. W. Cheong, and A. G. Dempster, "A DSRC doppler/IMU/GNSS tightly-coupled cooperative positioning method for relative positioning in VANETs," *J. Navigat.*, vol. 70, no. 1, pp. 120–136, 2017.
[22] M. Tahir, S. S. Afzal, M. S. Chughtai, and K. Ali, "On the accuracy of intervehicular range measurements using GNSS observables in a cooperative framework," *IEEE Trans. Intell. Transp. Syst.*, vol. 20, no. 2, pp. 682–691, Feb. 2019.
[23] D. Yang, F. Zhao, K. Liu, H. B. Lim, E. Frazzoli, and D. Rus, "A GPS pseudorange based cooperative vehicular distance measurement technique," in *Proc. IEEE 75th Veh. Technol. Conf.*, May 2012, pp. 1–5.
[24] J. Y. Wee, "Vehicular ranging system and method of operation," U.S. Patent 9,897,700, Feb. 20 2018.
[25] A. Minetto, C. Cristodaro, and F. Dovis, "A collaborative method for GNSS-based inter-agent range estimation and hybrid positioning algorithm in harsh environment," in *Proc. 30th Int. Tech. Meeting Satell. Div. Inst. Navigat.,* 2017, pp. 3784–3795.
[26] E. D. Kaplan and C. Hegarty, *Understanding GPS/GNSS: Principles and Applications*. Norwood, MA, USA: Artech House, 2017.
[27] P. Misra and P. Enge, *Global Positioning System: Signals, Measurements and Performance*, 2nd ed. Lincoln, MA, USA: Ganga-Jamuna Press, 2006.
[28] J. Chaffee and J. Abel, "GDOP and the Cramer-Rao bound," in *Proc. IEEE Position, Location Navigat. Symp.*, Apr. 1994, pp. 663–668.
[29] A. Minetto and F. Dovis, "A theoretical framework for collaborative estimation of distances among GNSS users," in *Proc. IEEE/ION Position, Location Navigat. Symp.*, Apr. 2018, pp. 1492–1501.

Alex Minetto is currently working toward the Ph.D. degree with the Politecnico di Torino, Turin, Italy, within the Navigation Signal Analysis and Simulation Group. He completed his master's thesis at European Organization for the Exploitation of Meteorological Satellites (EUMETSAT), Darmstadt, Germany, addressing the development of a new precise detection algorithm for radar pulses sent from Metop satellites during their calibration campaign. His research is focused on GNSS-based cooperative positioning algorithms.

Fabio Dovis is currently an Associate Professor with the Department of Electronics and Telecommunications, Politecnico di Torino, Turin, Italy, and also a member of the Navigation Signal Analysis and Simulation Group. His research interests cover the design of GPS and Galileo receivers and advanced signal processing for interference and multipath detection and mitigation. He has a relevant experience in European projects in satellite navigation as well as cooperation with industries and research centers.